

2014

Rational maps: the structure of Julia sets from accessible Mandelbrot sets

<https://hdl.handle.net/2144/15111>

"Downloaded from OpenBU. Boston University's institutional repository."

BOSTON UNIVERSITY
GRADUATE SCHOOL OF ARTS AND SCIENCES

Dissertation

**RATIONAL MAPS: THE STRUCTURE OF JULIA SETS
FROM ACCESSIBLE MANDELBROT SETS**

by

ELIZABETH L. FITZGIBBON

M.S., Long Island University C. W. Post, 2005
B.A., Long Island University C. W. Post, 2002

Submitted in partial fulfillment of the
requirements for the degree of
Doctor of Philosophy

2014

© Copyright by
ELIZABETH L. FITZGIBBON
2014

Approved by

First Reader

Robert L. Devaney, PhD
Professor of Mathematics

Second Reader

Paul Blanchard, PhD
Professor of Mathematics

Third Reader

Glen R. Hall, PhD
Professor of Mathematics

Acknowledgments

I would like to sincerely thank my advisor, Bob Devaney, for his support, guidance, and generosity of time over the last few years. I would also like to thank my committee, Paul Blanchard, Dick Hall, Gene Wayne, and Margaret Beck. I have enjoyed working with and learning from each of you. The Boston University Department of Mathematics & Statistics has provided an inspiring and collaborative environment. I have been fortunate to study with many talented classmates. Special thanks to my officemates, Rocio and Ava, for your support in all forms: intellectual, emotional, and edible. Finally, many thanks to Laurie, Kyle, and all of my family, especially my mother, Anne Fitzgibbon, for their unwavering support, encouragement, and understanding while I pursued my degree.

**RATIONAL MAPS: THE STRUCTURE OF JULIA SETS
FROM ACCESSIBLE MANDELBROT SETS**

(Order No.)

ELIZABETH L. FITZGIBBON

Boston University, Graduate School of Arts and Sciences, 2014

Major Professor: Robert L. Devaney, Professor of Mathematics

ABSTRACT

For the family of complex rational maps $F_\lambda(z) = z^n + \frac{\lambda}{z^d}$, where λ is a complex parameter and $n, d \geq 2$ are integers, many small copies of the well-known Mandelbrot set are visible in the parameter plane. An infinite number of these are located around the boundary of the connectedness locus and are accessible by parameter rays from the Cantor set locus. Maps taken from main cardioid of these accessible Mandelbrot sets have attracting periodic cycles. A method for constructing models of the Julia sets corresponding to such maps is described. These models are then used to explore the existence of dynamical conjugacies between maps taken from distinct accessible Mandelbrot sets in the upper halfplane.

Contents

1	Introduction	1
1.1	Singularly Perturbed Complex Polynomials	1
1.2	Checkerboard Julia Sets	4
1.3	Parameter Rays and Dynamical Rays	6
2	Structure of Julia Sets when $n = d = 2$	8
2.1	General Structure	8
2.2	Locating the Periodic Critical Point	13
2.3	Constructing Models	14
2.3.1	The Period-2 Case	14
2.3.2	The Period-3 Case	18
2.4	Uniqueness of the Itinerary	24
2.5	Conclusion	29
3	Construction of Models for $n = d \geq 3$	31
3.1	Locating Periodic Critical Points	31
3.2	An Example with $n = d = 3$ and t odd	32
3.3	An Example with $n = d = 3$ and t even	34
3.4	Symmetries in the Parameter Plane	35
	Bibliography	40

List of Figures

1.1	The parameter plane for $n = d = 4$	3
1.2	A Checkerboard Julia set corresponding to $\lambda = 0.15$ with $n = d = 4$ and a magnification.	5
1.3	External rays in the parameter plane for $n = d = 2$	7
2.1	The Julia set for λ taken from the $\frac{1}{3}$ -Mandelbrot set when $n = d = 2$ and a magnification of sector I_1	9
2.2	A model of the dynamical plane for λ taken from the $\frac{1}{3}$ -Mandelbrot set when $n = d = 2$	11
2.3	A model of the dynamical plane for λ taken from the $\frac{1}{3}$ -Mandelbrot set when $n = d = 2$	16
2.4	The chain of preimages of T_λ for λ taken from the $\frac{1}{3}$ -Mandelbrot set when $n = d = 2$. The highlighted portion of ∂I_{23}^{-1} maps to the high- lighted portion of ∂I_3 under F_λ	17
2.5	Locating the corners of T_{31}^{-2} and T_{311}^{-3} for λ taken from the $\frac{2}{7}$ -Mandelbrot set when $n = d = 2$. In the top figure, the highlighted portion of ∂I_{31}^{-1} maps onto the highlighted portion of ∂I_1 . In the bottom figure, the highlighted portion of ∂I_{311}^{-2} maps onto the highlighted portion of ∂I_{11}^{-1}	20
2.6	The final chain of preimages of T_λ for λ taken from the $\frac{2}{7}$ -Mandelbrot set when $n = d = 2$	21

2.7	The dynamical planes and the corresponding Julia set models for maps taken from the $\frac{1}{7}$, $\frac{2}{7}$, and $\frac{3}{7}$ -Mandelbrot sets, respectively, when $n = d = 2$. At first glance, these Julia sets may appear homeomorphic. Comparison of their models clearly shows that this is not the case. . . .	23
2.8	A model of the dynamical plane for λ taken from the $\frac{6}{15}$ Mandelbrot set when $n = d = 2$	25
2.9	For the $\frac{1}{7}$ -Mandelbrot set, we use fourfold symmetry to extend the chain of preimages of the trapdoor into the other symmetry sectors. . .	28
2.10	Given a model without the corresponding itinerary, we note that c_0 lies in I_{0312}^{-3} . Thus, c_2 is periodic with itinerary $\overline{231}$	28
3.1	The Julia set for λ taken from the $\frac{1}{26}$ -Mandelbrot set when $n = 3$. . .	33
3.2	The model of the Julia set for λ taken from the $\frac{1}{26}$ -Mandelbrot set when $n = 3$	34
3.3	The Julia set for λ taken from the $\frac{2}{26}$ -Mandelbrot set when $n = 3$. . .	35
3.4	The model of the Julia set for λ taken from the $\frac{2}{26}$ -Mandelbrot set when $n = 3$	36
3.5	The parameter plane for $n = d = 4$. In the first image, arrows in the indicate dynamical conjugacies between maps taken from the centers of the main cardioids of the indicated period-2 accessible Mandelbrot sets. These conjugacies are given by complex conjugation and rotations. In the second image, we indicate all twelve period-2 accessible Mandelbrot sets. These comprise two conjugacy classes, one marked with circles and the other with hexagons.	37

3.6 The parameter plane for $n = d = 5$. In the first image, arrows in the indicate dynamical conjugacies between maps taken from the centers of the main cardioids of the indicated period-2 accessible Mandelbrot sets. These conjugacies are given by complex conjugation and rotations. In the second image, we indicate all twenty period-2 accessible Mandelbrot sets and the five associated conjugacy classes. 39

List of Symbols

$F_\lambda^{n,d} = F_\lambda$	the map given by $z \mapsto z^n + \frac{\lambda}{z^d}$
$J(F_\lambda)$	the Julia set of F_λ
B_λ	immediate basin of attraction of the fixed critical point at infinity
T_λ	trapdoor (preimage of B_λ containing zero)
$c_i^\lambda = c_i$	i^{th} critical point encountered as one moves counterclockwise around the critical circle starting from the positive real axis
C_i	connecting Fatou component containing c_i
$I_i^\lambda = I_i$	i^{th} symmetry sector
$I_{s_0 s_1 \dots s_k}^{-k}$	k^{th} preimage of I_{s_k} contained within $I_{s_0 s_1 \dots s_{k-1}}^{-k+1}$
$S(c_i)$	itinerary of c_i with respect to the symmetry sectors
$T_{s_0 s_1 \dots s_{k-1}}^{-k}$	k^{th} preimage of T_λ contained within $I_{s_0 s_1 \dots s_{k-1}}^{-k+1}$
R_θ	straight ray in exterior of unit disk, $\{z : z = te^{2\pi i\theta}, t > 1\}$
ϕ_λ	Böttcher coordinate used to define dynamical rays
Φ	homeomorphism used to define parameter rays
h_λ	homeomorphism taking $J(F_\lambda)$ to its model
$\theta(\lambda)$	the angle associated to the parameter ray landing on the cusp of the accessible Mandelbrot set containing λ
$\theta(F_\lambda^k(C_i))$	the angle associated to the dynamical ray landing on the Fatou component containing $F_\lambda^k(c_i)$

Chapter 1

Introduction

1.1 Singularly Perturbed Complex Polynomials

There has been much work in recent years to understand the dynamics of the family of rational maps on the Riemann sphere, $\overline{\mathbb{C}}$, of the form

$$F_\lambda(z) = z^n + \frac{\lambda}{z^d} \tag{1.1.1}$$

with $n \geq 2$, $d \geq 1$, and λ a complex parameter. The Julia set of such a map is often known to be a Sierpiński curve [2]. Cases for which this is true include: when the critical orbit enters the immediate basin of infinity after two or more iterations, when the parameter lies in the main cardioid of a buried baby Mandelbrot set, or when the parameter lies on a buried point in a Cantor necklace. When a critical point lies in the immediate basin of attraction of a fixed point, the map has a Checkerboard Julia set [1]. In the case of a Misiurewicz-Sierpiński map, where the critical points are strictly pre-periodic to a repelling cycle, the Julia set is known to be a generalized Sierpiński gasket [6].

In this paper, we will consider the case where a critical point lies in the immediate basin of attraction of a periodic point. First, we explore the structure of the Julia sets associated to such maps. Then, for fixed n and d , we ask whether two maps,

F_λ and F_μ , each with a critical point lying in the immediate basin of attraction of a point with period m will have conjugate dynamics on their Julia sets.

For simplicity, we consider here only the cases with $n = d$, thus

$$F_\lambda(z) = z^n + \frac{\lambda}{z^n}. \quad (1.1.2)$$

When $\lambda = 0$ the map is just the degree- n map, $F_\lambda(z) = z^n$, with a fixed critical point at 0. When $\lambda \neq 0$, the degree of the map doubles to $2n$ and 0 becomes a pole. Then there is a super-attracting critical point at infinity and $2n$ finite critical points located at the $2n^{\text{th}}$ roots of λ . There are, however, only two critical values, $v_\lambda = \pm 2\sqrt{\lambda}$. When n is even, $\pm v_\lambda$ both map onto the same point. When n is odd, the orbits of $\pm v_\lambda$ behave symmetrically with respect to $z \mapsto -z$ under iteration. Thus, we say that there is really only one *free critical orbit*.

The *Julia set* of F_λ , denoted by $J(F_\lambda)$, is defined as the closure of the set of repelling periodic points of F_λ . The complement of the Julia set is called the *Fatou set*. Components of the Fatou set may be *escaping* or *non-escaping*. That is, orbits of points in the Fatou set may eventually escape to infinity or they may be bounded for all time.

There is an open Fatou component containing infinity that maps n -to-1 onto itself. We call this region the *immediate basin of attraction* and denote it B_λ . F_λ is conjugate to z^n on B_λ . Since 0 maps onto infinity, there is an open Fatou component containing 0 which also maps n -to-1 onto B_λ . When this region is disjoint from B_λ , we call it the *trapdoor* and denote it T_λ .

We may partition the parameter plane into subsets according to the location of the associated critical values with respect to the sets B_λ and T_λ . The following theorem, from [7], describes all possible cases for which the critical orbit escapes to

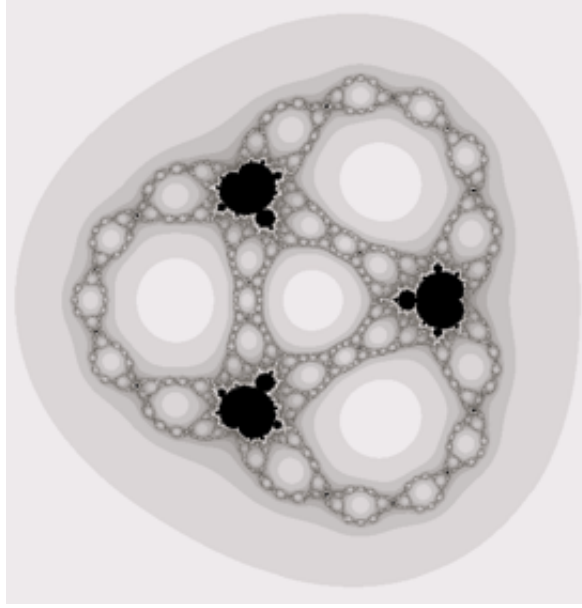


Figure 1.1: The parameter plane for $n = d = 4$.

infinity.

Theorem (The Escape Trichotomy)

Let v_λ be a critical value of F_λ .

1. If $v_\lambda \in B_\lambda$, then $J(F_\lambda)$ is a Cantor set of points.
2. If $T_\lambda \neq B_\lambda$ and $v_\lambda \in T_\lambda$, then $J(F_\lambda)$ is a Cantor set of concentric simple closed curves surrounding the origin. (This does not occur when $n = 2$.)
3. Otherwise, $J(F_\lambda)$ is a connected set. In particular, if $T_\lambda \neq B_\lambda$ and $F_\lambda^i(v_\lambda) \in T_\lambda$ for some $i \geq 1$, then $J(F_\lambda)$ is a Sierpiński curve.

To illustrate this, we display the parameter plane for $n = d = 4$ in Figure 1.1. The exterior grey region containing infinity is called the *Cantor set locus* and corresponds to the first part of the theorem. The light grey region at the center containing $\lambda = 0$

is called the *McMullen domain* and corresponds to the second part of the theorem. The additional light grey regions are called *Sierpiński holes* and correspond to the Sierpiński curve Julia sets described in the third part of the theorem.

Also observed in numerically generated diagrams of the parameter plane are small copies of the well-known *Mandelbrot set*. In many cases, standard arguments using polynomial-like maps (such as in [4]) prove the existence of such baby Mandelbrot sets. When λ is chosen from one of these baby Mandelbrot sets, the critical orbit does not escape to infinity and the third part of the Escape Trichotomy tells us that the Julia set is connected. Some of these baby Mandelbrot sets are *buried*, that is, they do not touch the Cantor set locus. Julia sets of maps taken from the main cardioids of one of these buried Mandelbrot sets are known to be Sierpiński curves [5]. In this paper, we investigate the structure of Julia sets corresponding to parameters from the *accessible* baby Mandelbrot sets, whose cusps are located along the boundary of the Cantor set locus.

1.2 Checkerboard Julia Sets

We observe that in each parameter plane with $n = d > 2$, there are $n - 1$ *principal* accessible Mandelbrot sets [3]. For example, when $n = d = 4$, as in Figure 1.1, we see three large copies of the Mandelbrot set. Maps taken from the main cardioids of these principal Mandelbrot sets are known to have *Checkerboard* Julia sets [1]. That is, the boundary of each non-escaping Fatou component (colored in black) touches infinitely many boundaries of escaping Fatou components (colored light grey), but it does not touch the boundary of any other non-escaping Fatou component. Similarly, the boundary of any escaping Fatou component touches infinitely many boundaries of non-escaping Fatou components, but it does not touch the boundary of any other

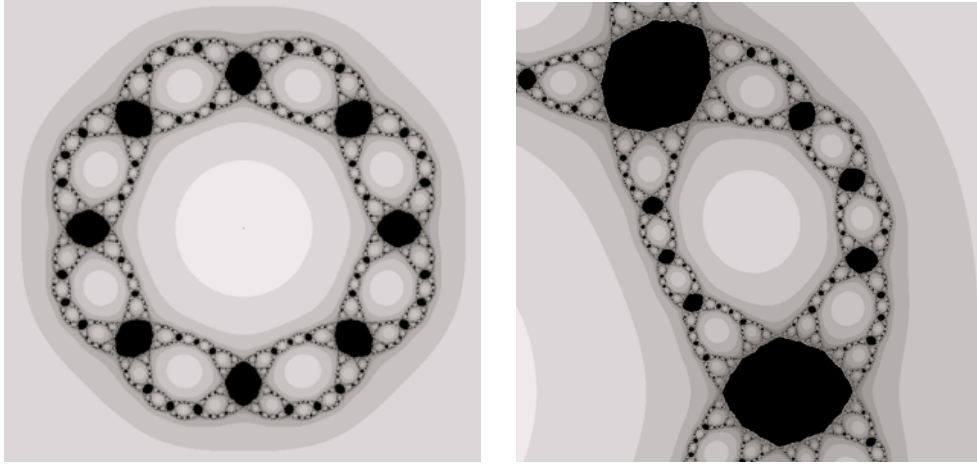


Figure 1.2: A Checkerboard Julia set corresponding to $\lambda = 0.15$ with $n = d = 4$ and a magnification.

escaping Fatou component, as shown in Figure 1.2. When $n = d = 2$, we do not have exact copies of the Mandelbrot set, however, there is a large black cardioid-shaped region. Maps taken from this main cardioid also have Checkerboard Julia sets.

For $n = d \geq 2$, any two maps taken from different main cardioids of principal Mandelbrot sets have homeomorphic Julia sets. However, these maps will not necessarily exhibit conjugate dynamics. These facts, as well as a method of determining the exact number of conjugacy classes for such maps, are presented in [1].

If one zooms in on the boundary of the Cantor set locus, one notices additional smaller Mandelbrot sets located symmetrically between the principal Mandelbrot sets. In fact, it appears that there are infinitely many levels of progressively smaller accessible Mandelbrot sets. As in the Checkerboard case, we ask whether maps corresponding to distinct main cardioids from the same level of accessible Mandelbrot sets will have conjugate dynamics. In the case of $n = d = 2$, we will show that the answer is no, unless the accessible Mandelbrot sets are complex conjugates of one another.

1.3 Parameter Rays and Dynamical Rays

Consider the case where $n = d$. Just as in the case of the complex quadratic map, there exists a unique conformal homeomorphism Φ which takes parameters in the Cantor set locus to points in $\overline{\mathbb{C}} - \overline{\mathbb{D}}$. If we define straight rays in $\overline{\mathbb{C}} - \overline{\mathbb{D}}$ by $R_\theta = \{re^{2\pi i\theta} : r > 1, 0 \leq \theta < 1\}$, then we can define *external parameter rays* by $\Phi^{-1}(R_\theta)$.

To give an explicit representation of Φ , we make use of $\phi_\lambda : B_\lambda \rightarrow \overline{\mathbb{C}} - \overline{\mathbb{D}}$, a holomorphic map known as the Böttcher coordinate. ϕ_λ maps ∞ to itself and conjugates F_λ to the map $z \mapsto z^n$ on B_λ . We can define *dynamical rays* in B_λ as the inverse images of the straight rays, R_θ [9]. We then define $\Phi(\lambda) = n\phi_\lambda(F_\lambda(c_\lambda))$ where c_λ is any one of the four critical points. Since F_λ is hyperbolic on $J(F_\lambda)$, it is known that ∂B_λ is a simple closed curve and we can extend this homeomorphism to the boundary, $\phi_\lambda : \overline{B_\lambda} \mapsto \overline{\mathbb{C}} - \overline{\mathbb{D}}$.

In particular, the parameter rays having $\Phi(\lambda) \in R_\theta$ with $\theta = \frac{t}{2^m - 1}$ where $m = 2, 3, 4, \dots$ and $t = 1, 2, 3, \dots, 2^m - 2$, land on hyperbolic components containing parameters corresponding to maps with an orbit of period m [10]. We conjecture that these hyperbolic components are, in fact, main cardioids of baby Mandelbrot sets and the external rays land at the cusps of these cardioids. We refer to such a Mandelbrot set as the $\frac{t}{2^m - 1}$ -Mandelbrot set.

Maps taken from the same hyperbolic component are known to be quasiconformally conjugate on their Julia sets [8], thus any two parameters in the same main cardioid will have attracting periodic orbits of the same period. The unique λ in each main cardioid for which the critical orbit is super-attracting is called the *center* of the main cardioid. Thus the critical orbit of the map taken from the center of the $\frac{t}{2^m - 1}$ -Mandelbrot set has period m . We shall restrict our investigation to these points. As an example, the parameter plane and several external rays for $n = d = 2$

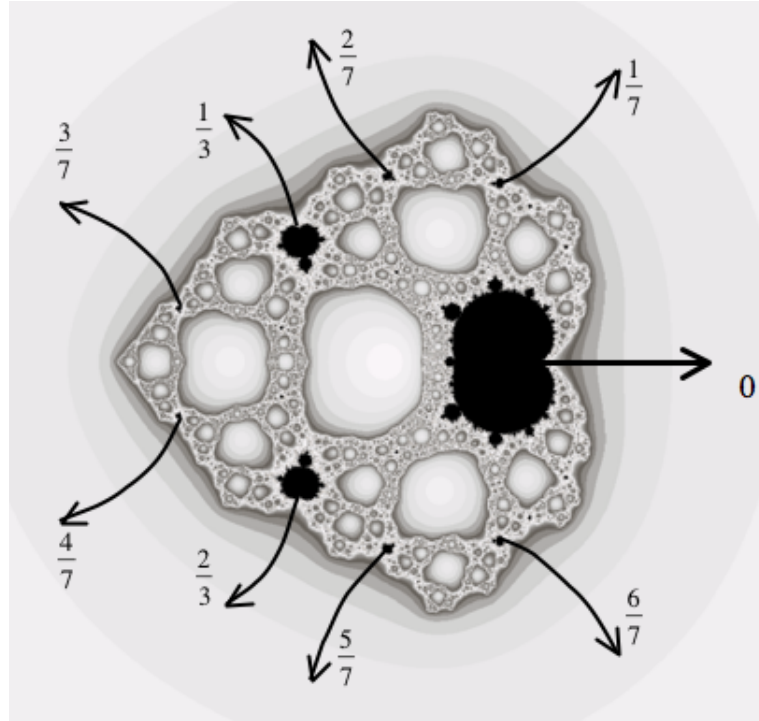


Figure 1.3: External rays in the parameter plane for $n = d = 2$.

are shown in Figure 1.3.

Note that $\overline{F_\lambda(z)} = F_{\bar{\lambda}}(\bar{z})$. Therefore, F_λ is dynamically conjugate to $F_{\bar{\lambda}}$ under complex conjugation and the Julia sets of these maps are homeomorphic. This allows us to further restrict our study to the upper-half of the parameter plane and we consider only λ at the centers of the main cardioids of the $\frac{t}{2^{m-1}}$ Mandelbrot sets with $t = 1, \dots, 2^{m-1} - 1$.

Chapter 2

Structure of Julia Sets when $n = d = 2$

2.1 General Structure

The map $F_\lambda(z) = z^2 + \frac{\lambda}{z^2}$ has degree 4 and has four finite critical points. When λ is the center of the main cardioid of an accessible Mandelbrot set, one of the four critical points is periodic. The remaining three critical points are pre-periodic and eventually land on the periodic critical orbit. Thus, each of the four critical points is located in a non-escaping Fatou component. To distinguish the four critical points, we define the *critical circle* by $\{z : |z| = |\lambda|^{\frac{1}{4}}\}$. Starting at the positive real axis, we move counterclockwise along the critical circle and label the critical points c_1 , c_2 , c_3 , and c_0 , in the order that they are encountered. We then let C_i denote the non-escaping Fatou component containing c_i .

Since $F_\lambda^2(z) = F_\lambda^2(iz)$, the Julia set has four-fold symmetry. We conclude that the critical points and corresponding C_i are located symmetrically at quarter-turn intervals about the origin.

By the Escape Trichotomy, we know that the Julia set is connected. Combined with fourfold symmetry, we conclude that B_λ is disjoint from T_λ . Furthermore, since all four critical points lie in non-escaping Fatou components, $\partial B_\lambda \cap \partial T_\lambda$ cannot contain a critical point, so ∂B_λ must be disjoint from ∂T_λ .

When λ is the cusp of the main cardioid of the $\frac{t}{2^m-1}$ Mandelbrot set, F_λ^m has

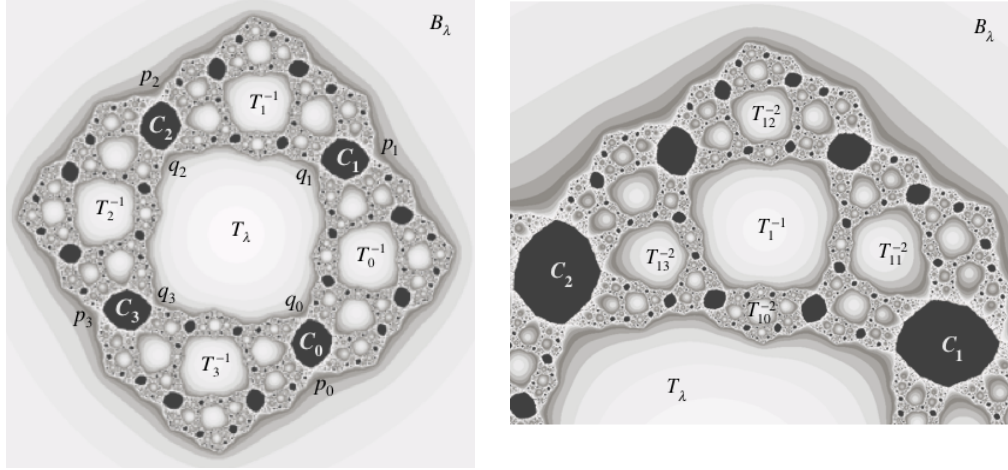


Figure 2.1: The Julia set for λ taken from the $\frac{1}{3}$ -Mandelbrot set when $n = d = 2$ and a magnification of sector I_1 .

a unique neutral fixed point located at the intersection of the boundary of a non-escaping Fatou component and ∂B_λ . Then, for the map taken from the center of the same main cardioid, the boundary of the C_i containing the periodic critical point c_i must intersect ∂B_λ at a point p_i . Since ∂T_λ maps onto ∂B_λ , the image of p_i under F_λ has a pre-image q_j which must be contained in $\partial T_\lambda \cap \partial C_j$, for some j . Therefore, each ∂C_i has a point, p_i , on ∂B_λ and another point, q_i , on ∂T_λ . For this reason, we call C_i a *connecting* Fatou component (see Figure 2.1).

F_λ maps B_λ two-to-one onto itself and also maps T_λ two-to-one onto B_λ . Since F_λ has degree 4, this accounts for all possible preimages of points in B_λ . Thus, any eventually escaping points not already located in B_λ must map through T_λ before escaping. (It is for this reason we call T_λ the *trapdoor*.) Since the critical orbit is assumed to be periodic, we know that the critical values cannot lie in any pre-image of T_λ , so these pre-images must map univalently onto T_λ . We conclude that there are four disjoint preimages of T_λ located symmetrically about the origin. We now

see that the dynamical plane can be divided into 4 symmetric sectors. Let the sector I_i be defined as the closed region whose boundary is given by the portions of ∂C_i , ∂B_λ , ∂C_{i+1} , and ∂T_λ that are traced out as one moves counterclockwise from p_i to p_{i+1} to q_{i+1} to q_i and back to p_i in such a way that C_i is included in the interior of I_i .

As proven in [1], F_λ maps each I_i univalently (except at the junction points) over the region that is the complement of the three sets B_λ , $F_\lambda(C_i)$, and $F_\lambda(C_{i+1})$. More specifically, the portion of ∂B_λ in I_i is mapped to half of ∂B_λ , while the portion of ∂T_λ in I_i is mapped to the remaining half of ∂B_λ . By this result it suffices to focus on only one I_i to understand the entire $J(F_\lambda)$.

Since ∂T_λ intersects the boundaries of four connecting Fatou components, the boundary of each preimage of T_λ must intersect the boundary of a preimage of each of these four connecting Fatou components. We call these Fatou components the *corners* of the preimage of T_λ . We've assumed one C_i with period $m \geq 2$ and all others eventually with period m , so no C_i can be its own preimage. Also $F_\lambda(C_1) = F_\lambda(C_3) = -F_\lambda(C_0) = -F_\lambda(C_2)$. Therefore, if C_1 maps onto C_2 , then C_0 maps onto itself, a contradiction. By similar arguments, we see that no C_i can be the preimage of any other because this would imply that at least one is fixed. Therefore, all preimages of the C_i are disjoint from the C_i . Furthermore, the order of the preimages of the C_i , as one travels counterclockwise around the boundary of the preimage of T_λ , must be the same as the order of the C_i themselves. Thus, each sector can be divided into four subsectors. For $k \geq 1$, we denote a k^{th} preimage of T_λ by $T_{s_0 \dots s_{k-1}}^{-k}$, where $s_j = 0, 1, 2,$ or 3 identifies the sector in which the j^{th} image of $T_{s_0 \dots s_{k-1}}^{-k}$ lands.

We show an example of a Julia set for a map taken from the main cardioid of

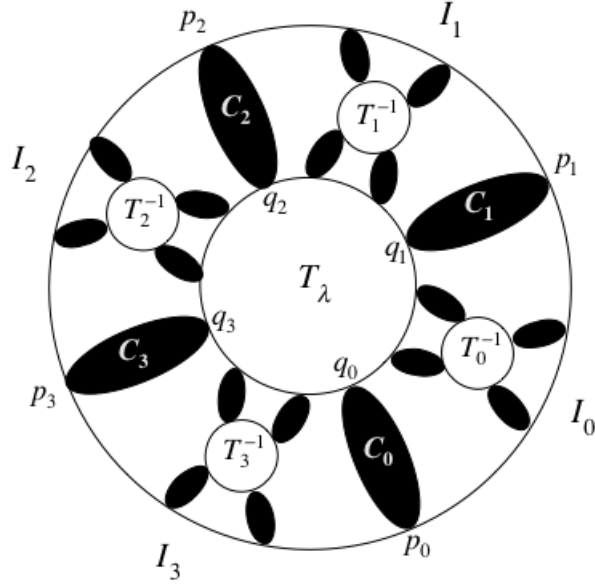


Figure 2.2: A model of the dynamical plane for λ taken from the $\frac{1}{3}$ -Mandelbrot set when $n = d = 2$.

the $\frac{1}{3}$ -Mandelbrot set in Figure 2.1 and a model of the dynamical plane for the same map in Figure 2.2.

The following Lemmas are useful in describing the dynamical plane.

Lemma 1: There cannot be more than four connecting Fatou components.

Proof Without loss of generality, suppose a fifth connecting component, C_4 , exists within the preimage of sector I_1 contained in sector I_0 . Note that C_4 does not contain a critical point. As mentioned earlier, $\partial I_0 \cap \partial B_\lambda$ maps to half of ∂B_λ and $\partial I_0 \cap \partial T_\lambda$ maps to the other half of ∂B_λ . Thus the points p_4 and q_4 , must map to distinct points in $\partial I_1 \cap \partial B_\lambda$ which lie on opposite sides of the point $F_\lambda(p_1) = F_\lambda(q_1)$. Since ∂B_λ is invariant under F_λ , all forward images of p_4 and q_4 lie in ∂B_λ . All black Fatou components are preimages of the periodic C_i (where $i = 0, 1, 2$, or 3), so there is some minimal k for which $F^k(C_4) = C_i$. C_i intersects ∂B_λ at a single point, p_i . Thus

$F_\lambda^k(p_4) = F_\lambda^k(q_4) = p_i$. But C_4 and its first $k - 1$ images cannot contain a critical point, so $F_\lambda^{k-1}(C_4)$ must map univalently onto C_i . Therefore, $F_\lambda^k(p_4) \neq F_\lambda^k(q_4)$, a contradiction. \square

Lemma 2: Let λ be the center of the main cardioid of an accessible Mandelbrot set with critical orbit of period $m \geq 2$. Then $T_{s_0 s_1 \dots s_{k-1}}^{-k}$ (with $1 \leq k \leq m$ and $s_j = 0, 1, 2$, or 3) cannot have all four corners lying on ∂B_λ , nor can $T_{s_0 s_1 \dots s_{k-1}}^{-k}$ have exactly three corners lying on ∂B_λ .

Proof By the assumptions $m \geq 2$ and $1 \leq k \leq m$, the corners of $T_{s_0 s_1 \dots s_{k-1}}^{-k}$ must be different from C_{s_0} and C_{s_0+1} . Suppose there exists $T_{s_0}^{-1}$ with all four corners on $\partial B_\lambda \cap \partial I_{s_0}$. Since $\partial B_\lambda \cap \partial I_{s_0}$ maps to half of ∂B_λ , the images of the four corners of $T_{s_0}^{-1}$, namely the C_i , must all lie on the same half of ∂B_λ . This violates the fourfold symmetry discussed earlier. Now suppose there exists a $T_{s_0 s_1}^{-2}$ having four corners on ∂B_λ , then its image, namely $T_{s_1}^{-1}$, must also have four corners on ∂B_λ , but we have shown that this is not possible. Continue inductively. A similar argument will show that $T_{s_0 s_1 \dots s_{k-1}}^{-k}$ cannot have exactly three corners on $\partial B_\lambda \cap \partial I_{s_0}$. \square

Lemma 3: For λ at the center of the main cardioid of an accessible Mandelbrot set with critical orbit of period greater than or equal to 2, there is exactly one region in each I_i with two corners lying on ∂B_λ and two corners lying on ∂T_λ . Such a region must be T_i^{-1} .

Proof Suppose there is a region in I_i with the same structure as T_i^{-1} . Then its image under F_λ will have four corners on ∂B_λ but will be different from T_λ . However, by Lemma 2, there are no such regions. \square

2.2 Locating the Periodic Critical Point

Lemma 4: For $n = d = 2$, if λ is taken from the center of the main cardioid of the $\frac{t}{2^m-1}$ accessible Mandelbrot set, then c_{t+1} is the periodic critical point.

Proof We will denote by $\theta(F_\lambda^k(C_i))$ the angle corresponding to the dynamical ray landing on the Fatou component containing $F_\lambda^k(c_i)$. Because it will cause no confusion, we similarly denote by $\theta(\lambda)$ the angle of the parameter ray landing on the accessible Mandelbrot set whose center is given by λ . We defined the parameter rays by $\Phi(\lambda) = 2\phi_\lambda(F_\lambda(c_\lambda))$. Since ϕ_λ conjugates F_λ to $z \mapsto z^2$ on B_λ , we know that $\theta(F_\lambda^k(C_i)) = 2^k\theta(C_i)$ and thus $\theta(\lambda) = 4\theta(C_i)$. This implies that $\theta(C_1) = \frac{t}{4(2^m-1)}$. In general,

$$\theta(C_i) = \frac{t}{4(2^m-1)} + \frac{i-1}{4} = \frac{t + (i-1)(2^m-1)}{4(2^m-1)}.$$

We can then compute the angle corresponding to the dynamical ray landing on the Fatou component containing $F_\lambda^m(C_i)$,

$$\theta(F_\lambda^m(c_i)) = 2^m \left(\frac{t + (i-1)(2^m-1)}{4(2^m-1)} \right).$$

If $\theta(F_\lambda^m(c_i)) \equiv \theta(c_i) \pmod{1}$ (equivalently, if $\theta(F_\lambda^m(c_i)) - \theta(c_i) \in \mathbb{Z}$), then c_i has period- m under F_λ .

Suppose $i = t + 1$ and consider $\theta(F_\lambda^m(c_i)) - \theta(c_i)$

$$\begin{aligned} &= \frac{2^m(t + ((t+1) - 1)(2^m - 1))}{4(2^m - 1)} - \frac{t + ((t+1) - 1)(2^m - 1)}{4(2^m - 1)} \\ &= \frac{(2^m - 1)(t + t(2^m - 1))}{4(2^m - 1)} \\ &= \frac{2^m t}{4} \end{aligned}$$

$$= 2^{m-2}t.$$

Since $m \geq 2$ and t is an integer, we see that $2^{m-2}t \in \mathbb{Z}$, so c_{t+1} has period- m under F_λ . We know that all four of the c_i map onto the same point after two iterations, so c_{t+1} is the only periodic c_i . \square

2.3 Constructing Models

If the maps F_λ and F_μ have conjugate dynamics on their Julia sets, we should be able to define a homeomorphism between $J(F_\lambda)$ and $J(F_\mu)$. Furthermore, we expect to find a homeomorphism that takes ∂B_λ to ∂B_μ and ∂T_λ to ∂T_μ . In the argument below, we construct a basic model for the structure of the Julia set and show that no such homeomorphism can exist between two such models, unless the main cardioids with centers λ and μ are complex conjugates of one another.

We remark that the case where all critical points of F_λ are strictly pre-periodic and lie in ∂B_λ was studied in [6]. Such maps are known as *Misiurewicz-Sierpiński* maps or, more succinctly, *MS* maps. The structure of the dynamical plane corresponding to an MS map is similar to the structure for maps with a periodic critical point. For this reason, we use much of the same notation and a similar method for constructing models of the associated Julia sets.

2.3.1 The Period-2 Case

As our first example, we begin with λ at the center of the main cardioid of the $\frac{1}{3}$ -Mandelbrot set, so $\theta(\lambda) = \frac{1}{3}$. Since $\frac{1}{3}$ has period 2 under the angle-doubling map, we know that one of the critical points of F_λ is periodic with period 2. We identify the connecting Fatou components containing the critical points down to single points which we continue to refer to as C_i . Likewise, we identify all preimages of the C_i

down to single points. From our computations in the proof of Lemma 4, we have $\theta(C_1) = \frac{1}{12}$. By Lemma 4, c_2 is known to be the periodic critical point and, in fact, $\theta(C_2) = \frac{4}{12}$ has period-2 under doubling.

Now, the portion of ∂B_λ that lies on the boundary of each I_i is associated to an interval on the unit circle. To avoid ambiguity, we take each C_i to lie in I_i but not in I_{i-1} . Thus:

$$z \in \partial B_\lambda \cap I_1 \implies \theta(z) \in \left[\frac{1}{12}, \frac{1}{3} \right)$$

$$z \in \partial B_\lambda \cap I_2 \implies \theta(z) \in \left[\frac{1}{3}, \frac{7}{12} \right)$$

$$z \in \partial B_\lambda \cap I_3 \implies \theta(z) \in \left[\frac{7}{12}, \frac{5}{6} \right)$$

$$z \in \partial B_\lambda \cap I_0 \implies \theta(z) \in \left[\frac{5}{6}, \frac{1}{12} \right).$$

∂B_λ is invariant under F_λ , so all points in the forward orbit of C_2 lie in ∂B_λ . We can now assign an *itinerary* to C_2 according to the behavior of $\theta(C_2)$ with respect to the aforementioned intervals on the unit circle. Recall that the forward orbit of the dynamical ray landing at C_2 under doubling was given by $\frac{1}{3} \mapsto \frac{2}{3} \mapsto \frac{1}{3}$. This tells us that $C_2 \in \partial I_2$, $F_\lambda(C_2) \in \partial I_3$, and $F_\lambda^2(C_2) = C_2 \in \partial I_2$. We define the itinerary of C_2 by $S(C_2) = \overline{23}$.

We now construct a *model* for $J(F_\lambda)$. Begin by defining a homeomorphism, $h_\lambda : \partial B_\lambda \rightarrow \mathbb{S}^1$ such that $h_\lambda(z) = e^{2\pi i \theta(z)}$. Then extend h_λ to take ∂T_λ to a simple closed curve contained in $\overline{\mathbb{D}}$, which intersects the unit circle exactly four times at $h_\lambda(C_1), h_\lambda(C_2), h_\lambda(C_3)$, and $h_\lambda(C_0)$. This divides our model into four regions corresponding to the sectors, I_i . We continue to extend h_λ to points within each of these sectors.

By Lemma 3, there is a preimage of T_λ in each I_i , which has two corners on ∂B_λ

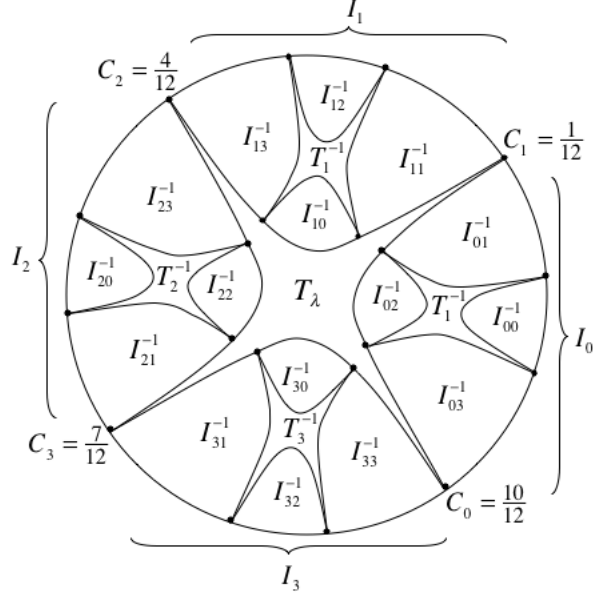


Figure 2.3: A model of the dynamical plane for λ taken from the $\frac{1}{3}$ -Mandelbrot set when $n = d = 2$.

and two corners on ∂T_λ . Using the angle-doubling map, we can compute precisely the angles associated to the corners of each $h_\lambda(T_i^{-1})$. We remark that $h_\lambda(F_\lambda(C_2)) = \frac{2}{3}$ corresponds to one of the corners where ∂T_3^{-1} intersects ∂B_λ .

The $h_\lambda(T_i^{-1})$ divide each $h_\lambda(I_i)$ into four subsectors which are preimages of the original four sectors. For simplicity and because it causes no confusion, we denote $h_\lambda(C_i)$ by C_i , $h_\lambda(I_i)$ by I_i , and $h_\lambda(T_i^{-1})$ by T_i^{-1} . We denote the preimage of I_j contained within I_i by I_{ij}^{-1} . Figure 2.3 depicts our model as described thus far.

Now each subsector must contain a $T_{s_0 s_1}^{-2}$, which has exactly two corners lying on $\partial T_{s_0}^{-1}$. We refer to the other two corners of $T_{s_0 s_1}^{-2}$ as the *free corners*. Since $F_\lambda^2(C_2) = C_2$, one of the free corners of T_{23}^{-2} must be C_2 . The other free corner of T_{23}^{-2} must lie in $\partial I_{23}^{-1} \cap (\partial B_\lambda \cup \partial T_\lambda)$.

To determine the specific location of this corner, we recall that F_λ preserves orientation of points along any preimage of ∂B_λ . This allows us to compare the

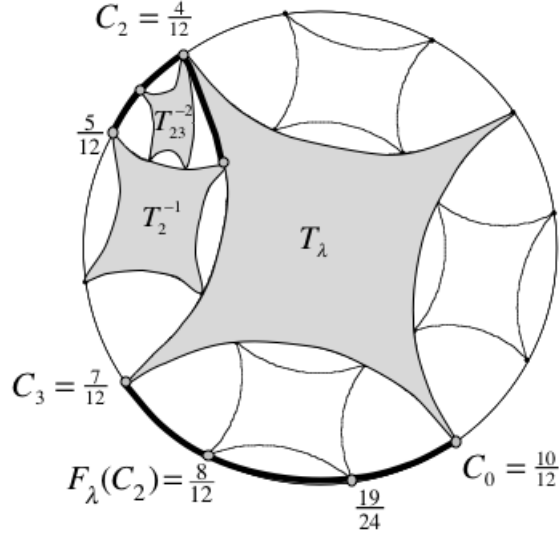


Figure 2.4: The chain of preimages of T_λ for λ taken from the $\frac{1}{3}$ -Mandelbrot set when $n = d = 2$. The highlighted portion of ∂I_{23}^{-1} maps to the highlighted portion of ∂I_3 under F_λ .

order of the free corners of T_{23}^{-2} along $\partial I_{23}^{-1} \cap (\partial B_\lambda \cup \partial T_\lambda)$ to the order of their forward images along ∂I_3 . The point where ∂T_2^{-1} intersects $\partial I_{23}^{-1} \cap \partial B_\lambda$ maps to $C_0 = \frac{5}{6}$, the point where ∂T_2^{-1} intersects $\partial I_{23}^{-1} \cap \partial T_\lambda$ maps to $C_3 = \frac{7}{12}$, and C_2 maps to $\frac{2}{3}$. Since the second free corner of T_3^{-1} lies between $\frac{2}{3}$ and $\frac{5}{6}$, we conclude that the second free corner of T_{23}^{-2} lies between the point where ∂T_2^{-1} intersects $\partial I_{23}^{-1} \cap \partial B_\lambda$ and the point C_2 . We now have a topological invariant, which we call a *chain of preimages* of T_λ . When the critical point c_i has period m and itinerary $S(c_i) = is_1 \dots s_{m-1}$, we consider a chain of preimages of T_λ to be the collection $\{T_\lambda, T_i^{-1}, T_{is_1}^{-2}, T_{is_1 s_2}^{-3}, \dots, T_{is_1 s_2 \dots s_{m-1}}^{-m}\}$.

The structure of T_{23}^{-2} and the chain of preimages of T_λ are illustrated in Figure 2.4. We observe that the structure of this model corresponds to the structure exhibited by the Julia set in Figure 2.1.

Consider the map F_μ associated to the parameter μ taken from the main cardioid of a different accessible Mandelbrot set. If there exists a homeomorphism between

$J(F_\lambda)$ and $J(F_\mu)$ which sends ∂B_λ to ∂B_μ and ∂T_λ to ∂T_μ , then the homeomorphism must preserve the structure of this chain of preimages of T_λ . It is clear that for any map with critical orbit of period m , the chain of preimages contains T_λ and m of its preimages. Therefore, since $\frac{1}{3}$ is the only period 2 angle in the upper halfplane, we immediately conclude that there is no such homeomorphism between the Julia set associated to a map from the $\frac{1}{3}$ -Mandelbrot set and the Julia set of a map taken from any other main cardioid in the upper halfplane. We recall, however, that maps taken from the $\frac{1}{3}$ -Mandelbrot set and maps taken from the $\frac{2}{3}$ -Mandelbrot set do have conjugate dynamics on their Julia sets.

2.3.2 The Period-3 Case

Next, we examine the three accessible Mandelbrot sets in the upper halfplane that have critical orbits of period 3. These are the $\frac{1}{7}$, $\frac{2}{7}$, and $\frac{3}{7}$ -Mandelbrot sets. We will see that the structure of the chain of preimages of T_λ is uniquely determined by the itinerary of the the periodic critical point which is, in turn, unique to the chosen Mandelbrot set.

Take, for example, λ at the center of the main cardioid of the $\frac{2}{7}$ -Mandelbrot set. Then $\theta(C_1) = \frac{2}{28}$. By symmetry, we compute that $\theta(C_2) = \frac{9}{28}$, $\theta(C_3) = \frac{4}{7}$, and $\theta(C_0) = \frac{23}{28}$. This again divides the unit circle into four intervals.

$$z \in \partial B_\lambda \cap I_1 \implies \theta(z) \in \left[\frac{1}{14}, \frac{9}{28} \right)$$

$$z \in \partial B_\lambda \cap I_2 \implies \theta(z) \in \left[\frac{9}{28}, \frac{4}{7} \right)$$

$$z \in \partial B_\lambda \cap I_3 \implies \theta(z) \in \left[\frac{4}{7}, \frac{23}{28} \right)$$

$$z \in \partial B_\lambda \cap I_0 \implies \theta(z) \in \left[\frac{23}{28}, \frac{1}{14} \right).$$

By Lemma 4, we know that c_3 is the periodic critical point. We now assign an itinerary to C_3 according to the behavior of $\theta(C_3)$ with respect to these four intervals. Recall that the forward orbit of the periodic dynamical ray landing at C_3 under doubling is given by $\frac{2}{7} \mapsto \frac{4}{7} \mapsto \frac{1}{7} \mapsto \frac{2}{7}$. This tells us that $C_3 \in \partial I_3$, $F_\lambda(C_3) \in \partial I_1$, $F_\lambda^2(C_3) \in \partial I_1$, and $F_\lambda^3(C_3) = C_3 \in \partial I_3$. We define the itinerary of C_3 as $S(C_3) = \overline{311}$. This itinerary will be useful in constructing the chain of preimages of T_λ in the model of $J(F_\lambda)$.

The chain will include T_λ , T_3^{-1} , T_{31}^{-2} , and T_{311}^{-3} . To give a full description of the structure of the chain, we determine the location of the corners of each element of the chain. We already know that the four corners of T_λ lie on ∂B_λ and that T_3^{-1} has two corners on ∂B_λ and two corners on ∂T_λ .

T_3^{-1} divides I_3 into four subsectors. T_{31}^{-2} is contained in I_{31}^{-1} and the four corners of T_{31}^{-2} lie on ∂I_{31}^{-1} . Exactly two corners of T_{31}^{-2} lie in ∂T_3^{-1} , so the two free corners of T_{31}^{-2} must lie in $\partial I_{31}^{-1} \cap (\partial B_\lambda \cup \partial T_\lambda)$. As in our previous example, the order of points along this curve is preserved under F_λ .

The point $\partial I_{31}^{-1} \cap \partial T_\lambda \cap \partial T_3^{-1}$ maps to C_1 . The free corners of T_{31}^{-2} map to the free corners of T_1^{-1} in ∂B_λ . C_3 maps to a point on the boundary of I_{11}^{-1} . $F_\lambda(C_3)$ lies between C_1 and the free corners of T_1^{-1} along the curve $\partial B_\lambda \cap \partial I_1$. Therefore, C_3 must lie between the point $\partial I_{31}^{-1} \cap \partial T_\lambda \cap \partial T_3^{-1}$ and the free corners of T_{31}^{-2} along the curve $\partial I_{31}^{-1} \cap (\partial B_\lambda \cup \partial T_\lambda)$, see Figure 2.5.

T_{311}^{-3} has two corners on ∂T_{31}^{-2} and two free corners which map onto the two free corners of T_{11}^{-2} . Since C_3 has period 3, one free corner of T_{311}^{-3} must be C_3 (in other words, C_3 is the preimage of one of the free corners of T_{11}^{-2}). It remains to find the location of the second free corner of T_{311}^{-3} , which must lie in $\partial I_{311}^{-2} \cap (\partial B_\lambda \cup \partial T_\lambda)$.

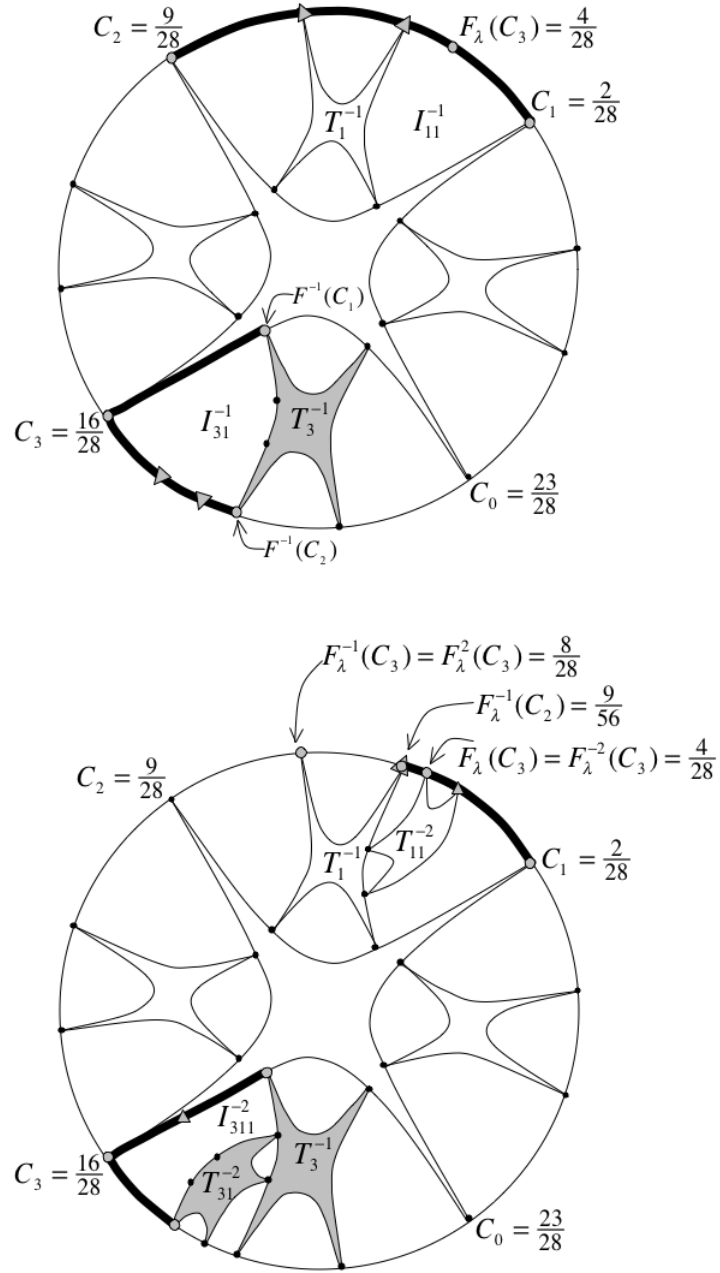


Figure 2.5: Locating the corners of T_{31}^{-2} and T_{311}^{-3} for λ taken from the $\frac{2}{7}$ -Mandelbrot set when $n = d = 2$. In the top figure, the highlighted portion of ∂I_{31}^{-1} maps onto the highlighted portion of ∂I_1 . In the bottom figure, the highlighted portion of ∂I_{311}^{-2} maps onto the highlighted portion of ∂I_{11}^{-1} .

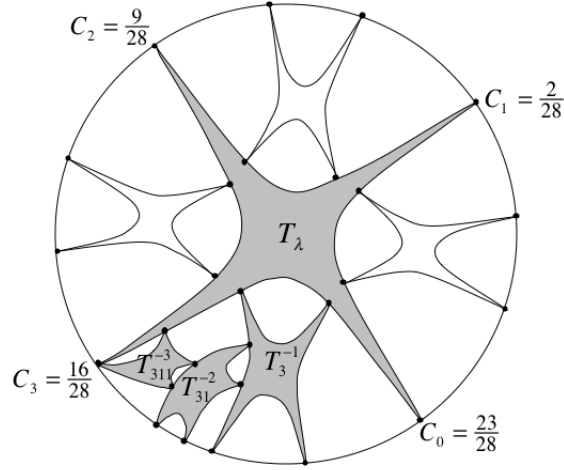


Figure 2.6: The final chain of preimages of T_λ for λ taken from the $\frac{2}{7}$ -Mandelbrot set when $n = d = 2$.

By symmetry, T_{11}^{-2} has the same structure as T_{31}^{-2} . This allows us to conclude that T_{11}^{-2} also has its two free corners on ∂B_λ . The free corners of T_{11}^{-2} then map onto the free corners of T_1^{-1} and the free corners of T_1^{-1} map onto C_2 and C_3 .

In particular, we note that we must move clockwise along $\partial B_\lambda \cap \partial I_1$ to get from $F^{-1}(C_2)$ to $F^{-1}(C_3)$ and clockwise along $\partial B_\lambda \cap \partial I_{11}^{-1}$ to get from $F^{-2}(C_2)$ to $F^{-2}(C_3)$. Similarly, we move clockwise along $\partial I_{311}^{-2} \cap (\partial B_\lambda \cup \partial T_\lambda)$ to get from $F^{-3}(C_3) = C_3$ to the second free corner of T_{311}^{-3} , see Figure 2.5. The complete chain of preimages of T_λ for this example is illustrated in Figure 2.6.

We then ask whether the chains of preimages of T_λ for maps taken from other accessible Mandelbrot sets with period 3 critical orbits will necessarily have the same structure. A quick glance at the numerically generated dynamical planes for maps taken from the $\frac{1}{7}$, $\frac{2}{7}$, and $\frac{3}{7}$ -Mandelbrot sets (see Figure 2.7) might suggest that a homeomorphism exists between their Julia sets. However, using the same method as before, we construct the chains of preimages of T_λ for the $\frac{1}{7}$ and $\frac{3}{7}$ -Mandelbrot sets. It is clear from the structures of these chains (also shown in Figure 2.7) that no

two of these maps can have homeomorphic Julia sets. We conclude that maps taken from the main cardioids of distinct accessible period-3 Mandelbrot sets cannot have conjugate dynamics on their Julia sets, unless these cardioids are complex conjugates of one another.

Next, we consider maps with critical orbits of period greater than 3. Our method for constructing chains will continue to prove useful. However, as the period increases, we see that constructing the chains becomes more complicated. In our previous examples, the free corners of each T^{-k} have fallen either on ∂B_λ or ∂T_λ , but this is not always the case. Sometimes, the free corners of a T^{-k} will fall on the boundary of some T^{-j} with $j < k$.

Take for example, λ at the center of the main cardioid of the $\frac{6}{15}$ -Mandelbrot set. Then $\theta(C_1) = \frac{1}{10}$, $\theta(C_2) = \frac{7}{20}$, $\theta(C_3) = \frac{2}{5}$, and $\theta(C_0) = \frac{17}{20}$. This again divides the unit circle into four intervals.

$$\begin{aligned} z \in \partial B_\lambda \cap I_1 &\implies \theta(z) \in \left[\frac{1}{10}, \frac{7}{20} \right) \\ z \in \partial B_\lambda \cap I_2 &\implies \theta(z) \in \left[\frac{7}{20}, \frac{3}{5} \right) \\ z \in \partial B_\lambda \cap I_3 &\implies \theta(z) \in \left[\frac{3}{5}, \frac{17}{20} \right) \\ z \in \partial B_\lambda \cap I_0 &\implies \theta(z) \in \left[\frac{17}{20}, \frac{1}{10} \right). \end{aligned}$$

By Lemma 4, we know that C_3 contains the periodic critical point. We compute the orbit of $\theta(C_3)$ under doubling: $\frac{3}{5} \mapsto \frac{1}{5} \mapsto \frac{2}{5} \mapsto \frac{4}{5} \mapsto \frac{3}{5}$. Thus, the periodic itinerary is given by $S(C_3) = \overline{3123}$.

C_3 must lie within I_{31}^{-1} , which implies that C_3 falls between the free corners of T_{31}^{-2} . Thus one free corner of T_{31}^{-2} lies on ∂B_λ and the other lies on ∂T_λ . C_3 must

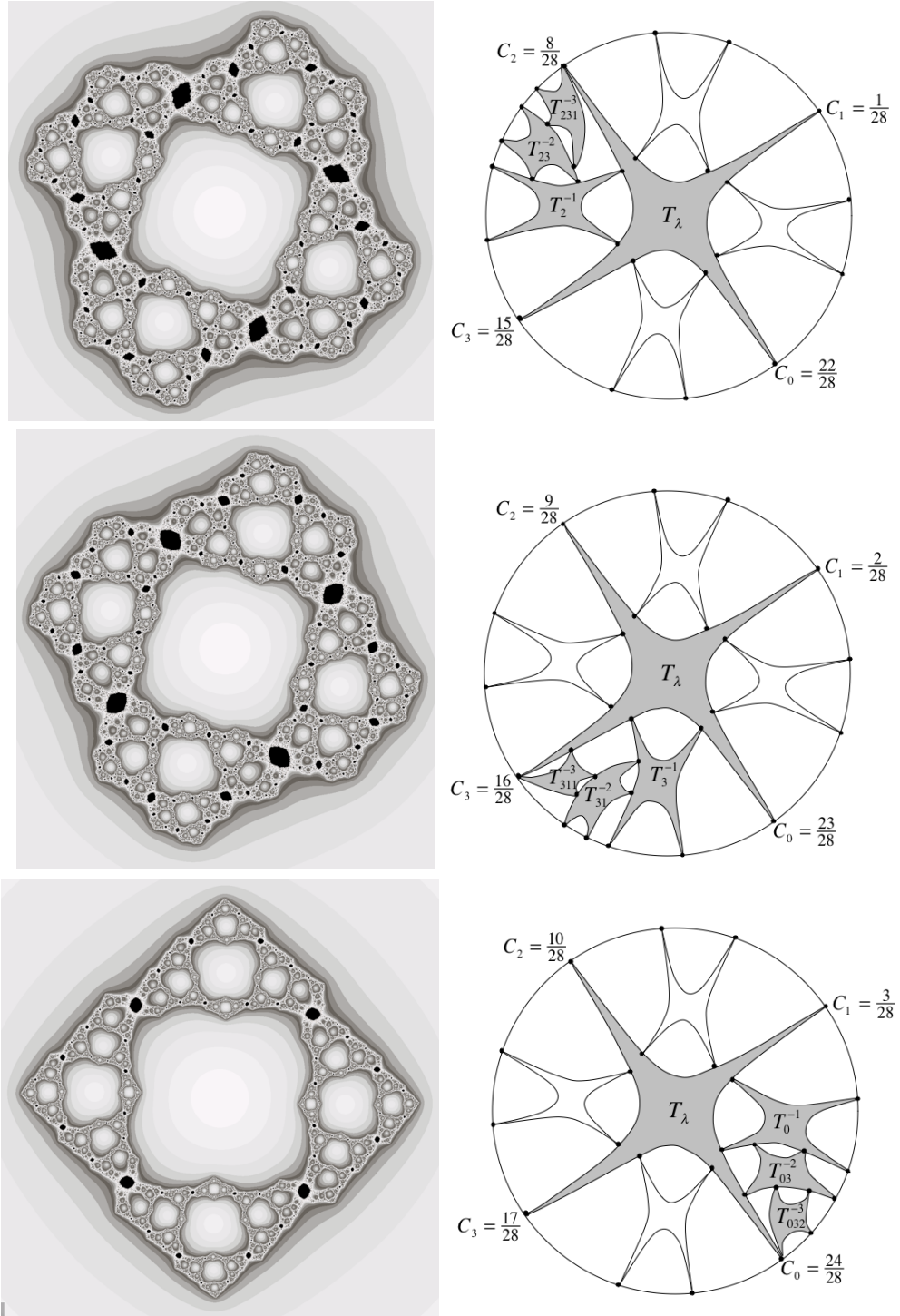


Figure 2.7: The dynamical planes and the corresponding Julia set models for maps taken from the $\frac{1}{7}$, $\frac{2}{7}$, and $\frac{3}{7}$ -Mandelbrot sets, respectively, when $n = d = 2$. At first glance, these Julia sets may appear homeomorphic. Comparison of their models clearly shows that this is not the case.

also lie within I_{312}^{-2} , which implies that both free corners of T_{312}^{-3} lie on ∂B_λ between C_3 and the free corner of T_{31}^{-2} that lies on ∂B_λ . So far, our method has progressed just as in our previous examples. Next, we know that C_3 is one corner of T_{3123}^{-4} and we need only find the location of a single free corner of T_{3123}^{-4} . This free corner lies on ∂I_{3123}^{-3} . Recall that each preimage of T_λ has exactly two corners on a previous preimage of T_λ , this implies that the free corner of T_{3123}^{-4} cannot lie in the section of ∂I_{3123}^{-3} that intersects ∂T_{312}^{-3} . Thus, the free corner lies either on $\partial B_\lambda \cap \partial I_{3123}^{-3}$ or $(\partial T_\lambda \cup \partial T_{31}^{-2}) \cap \partial I_{3123}^{-3}$. $F_\lambda^3(C_3)$ is the corner of T_3^{-1} in ∂T_λ closest to C_0 . This implies that the free corner of T_{3123}^{-4} lies in $(\partial T_\lambda \cup \partial T_{31}^{-2}) \cap \partial I_{3123}^{-3}$. To complete the model, we just determine whether this free corner lies on ∂T_λ or ∂T_{31}^{-2} . The point $\partial T_\lambda \cap \partial T_{31}^{-2}$ divides these two curve segments. By comparing the forward images of this point to the forward images of the free corner of T_{3123}^{-4} and using the fourfold symmetry of the Julia set, we can determine that the free corner lies on ∂T_{31}^{-2} . The model of this Julia set can be seen in Figure 2.8.

2.4 Uniqueness of the Itinerary

We have seen that the angle corresponding to an accessible Mandelbrot set can be used to construct a model for the Julia set corresponding to a map taken from the main cardioid of this Mandelbrot set. However, we now ask, is this model unique? That is, if we choose two different parameter rays generating two different itineraries, will the corresponding models be topologically distinct?

For example, we know that λ at the center of the $\frac{1}{3}$ -Mandelbrot set and $\bar{\lambda}$ at the center of the $\frac{2}{3}$ -Mandelbrot set give rise to topologically conjugate models under reflection through the real axis. The itinerary of the periodic critical point for λ is $S(c_2) = \overline{23}$ and the itinerary of the periodic critical point for $\bar{\lambda}$ is $S(c_3) = \overline{31}$. We

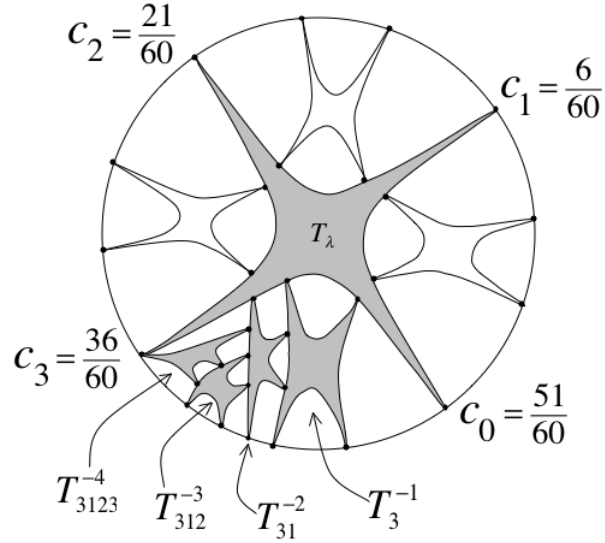


Figure 2.8: A model of the dynamical plane for λ taken from the $\frac{6}{15}$ Mandelbrot set when $n = d = 2$.

know that itineraries corresponding to complex conjugate parameters will necessarily be reflections of one another. So now we restrict to just the upper-halfplane and ask whether any two distinct itineraries can be rotations or reflections of one another.

Lemma 5: If λ and μ are the centers of distinct accessible Mandelbrot sets in the upper halfplane, then the itineraries generated by these parameters are distinct.

Proof: Suppose we can choose λ and μ , centers of distinct period- m accessible Mandelbrot sets in the upper halfplane, such that the periodic critical points of F_λ and F_μ generate the same itinerary. Let c_i^λ and c_i^μ with $i = 0, 1, 2, 3$, represent the critical points of F_λ and F_μ , respectively, where $\theta(c_1^\lambda), \theta(c_1^\mu) \in (0, \frac{1}{6})$. Likewise, let I_i^λ and I_i^μ represent the corresponding symmetry sectors. If $\theta(\lambda) = \frac{t}{2^m - 1}$, let $s_0 \equiv t + 1 \pmod{4}$ with $s_0 \in \{0, 1, 2, 3\}$. Then $c_{s_0}^\lambda$ is periodic under F_λ and its itinerary can be written $S(c_{s_0}^\lambda) = \overline{s_0 s_1 \dots s_{m-1}}$. This implies that $c_{s_0}^\mu$ is periodic under F_μ , so $\theta(c_{s_0}^\mu)$ must be of the form $\frac{t+4k}{2^m - 1}$ where $k \in \mathbb{Z}$ and $0 < k < 2^{m-3} - 1$. (Note that we need

only consider the cases of $m \geq 4$.) We can now define the angles of the dynamical rays corresponding to the critical points in the first quadrant by $\theta(c_1^\lambda) = \frac{t}{4(2^{m-1})}$ and $\theta(c_1^\mu) = \frac{t+4k}{4(2^{m-1})}$. The difference between these angles is $\frac{k}{2^{m-1}}$, which implies that the maximum difference between the angles corresponding to any point in I_1^λ and any point in I_1^μ is $\frac{1}{4} + \frac{k}{2^{m-1}}$. Thus, if $|\theta(F_\lambda^\eta(c_{s_0}^\lambda)) - \theta(F_\mu^\eta(c_{s_0}^\mu))| \in (\frac{1}{4} + \frac{k}{2^{m-1}}, \frac{3}{4} - \frac{k}{2^{m-1}})$, then $F_\lambda^\eta(c_{s_0}^\lambda)$ and $F_\mu^\eta(c_{s_0}^\mu)$ lie in different symmetry sectors and $S(c_{s_0}^\lambda) \neq S(c_{s_0}^\mu)$. We now show that such an $\eta \in 2, 3, \dots, m-1$ exists, in contradiction to our assumption. Since $0 < k < 2^{m-3} - 1$, we know that $\frac{k}{2^{m-1}} < \frac{1}{8}$ and $(\frac{3}{8}, \frac{5}{8}) \subset (\frac{1}{4} + \frac{k}{2^{m-1}}, \frac{3}{4} - \frac{k}{2^{m-1}})$. To compute $|\theta(F_\lambda^\eta(c_{s_0}^\lambda)) - \theta(F_\mu^\eta(c_{s_0}^\mu))|$, we need only follow the orbit of $\frac{k}{2^{m-1}}$ under doubling. Thus, it suffices to show that there exists an $\eta \in \{2, 3, \dots, m-1\}$ such that $\frac{2^\eta k}{2^{m-1}} \equiv x \pmod{1}$ such that $x \in (\frac{3}{8}, \frac{5}{8})$.

The angle $\frac{k}{2^{m-1}}$ has period- m under doubling: $\frac{2^m k}{2^{m-1}} = \frac{k}{2^{m-1}} + k \equiv \frac{k}{2^{m-1}} \pmod{1}$. We then consider preimages of this angle under doubling. We know that $\frac{k}{2^{m-1}} \in (0, \frac{1}{8})$, so $\frac{2^{m-1}k}{2^{m-1}} \pmod{1} \in (0, \frac{1}{16}) \cup (\frac{1}{2}, \frac{9}{16})$. If $\frac{2^{m-1}k}{2^{m-1}} \pmod{1} \in (\frac{1}{2}, \frac{9}{16}) \subset (\frac{3}{8}, \frac{5}{8})$, then we let $\eta = m-1$ and we're done. Otherwise, if $\frac{2^{m-1}k}{2^{m-1}} \pmod{1} \in (0, \frac{1}{16})$, we consider the subsequent preimage. Continuing inductively, if $\frac{2^{m-j+1}k}{2^{m-1}} \pmod{1} \in (0, \frac{1}{2^{j+2}})$, then $\frac{2^{m-j}k}{2^{m-1}} \pmod{1} \in (0, \frac{1}{2^{j+3}}) \cup (\frac{1}{2}, \frac{1}{2} + \frac{1}{2^{j+3}})$. For $j \geq 1$, $(0, \frac{1}{2^{j+3}}) \subset (0, \frac{1}{8})$ and $(\frac{1}{2}, \frac{1}{2} + \frac{1}{2^{j+3}}) \subset (\frac{3}{8}, \frac{5}{8})$. We cannot have $\frac{2^{m-j}k}{2^{m-1}} \pmod{1} \in (0, \frac{1}{8})$ for all $j = 1, 2, \dots, m-1$. So there must exist a $j \in \{1, 2, \dots, m-1\}$ such that $\frac{2^{m-j}k}{2^{m-1}} \pmod{1} \in (\frac{3}{8}, \frac{5}{8})$. We let $\eta = m-j$. \square

Lemma 6: The model for $J(F_\lambda)$ with λ taken from the center of a $\frac{t}{2^{m-1}}$ -Mandelbrot set corresponds to a unique itinerary.

Proof: One can determine the unique itinerary that generates a given model just by considering the location of any one of the critical points. Suppose c_{s_0} is a period- m critical point and has itinerary $S(c_{s_0}) = \overline{s_0 s_1 s_2 \dots s_{m-1}}$. Regardless of the choice of λ , the first iterate of each critical point always lands in a specified sector. For instance,

c_1 is always contained in I_{11}^{-1} . We also know that all four critical points map to the same point after two iterations, so the itineraries of the critical points are given by:

$$S(c_1) = 11s_2\dots s_{m-1}\overline{s_0s_1s_2\dots s_{m-1}}$$

$$S(c_2) = 23s_2\dots s_{m-1}\overline{s_0s_1s_2\dots s_{m-1}}$$

$$S(c_3) = 31s_2\dots s_{m-1}\overline{s_0s_1s_2\dots s_{m-1}}$$

$$S(c_0) = 03s_2\dots s_{m-1}\overline{s_0s_1s_2\dots s_{m-1}}$$

Thus, identifying the $I_{ij s_2 \dots s_m}^{-m}$ containing c_i , immediately tells us that c_{s_m} is the periodic critical point. Then the $I_{s_0 s_1 s_2 \dots s_m}^{-m}$ containing c_{s_m} , tells us that the itinerary of the periodic critical point must be $S(c_{s_0}) = \overline{s_0 s_1 s_2 \dots s_{m-1}}$. \square

As an example, consider the $\lambda = \frac{1}{7}$ case. We determined that c_2 was the periodic critical point and we constructed the chain of preimages of the trapdoor in Figure 2.7. We can now use the fourfold symmetry to extend this chain to the other sectors, as shown in Figure 2.9.

Now suppose we were given this model, without knowing the angle of the parameter ray corresponding to the accessible Mandelbrot set from which the parameter was taken. It is easy to determine the location of the periodic critical point, as well as the corresponding itinerary. We see that the chain of preimages of the trapdoor contains $T_\lambda, T^{-1}, T^{-2}$, and T^{-3} . Thus, we know the period of the critical orbit is 3. Now, we arbitrarily choose any of the critical points and consider its location within the preimages of the symmetry sectors. Notice, as indicated in Figure 2.10, that c_0 is contained in I_{0312}^{-3} . This tells us that, after 3 iterations, c_0 is mapped onto c_2 . So we conclude that c_2 is periodic. Furthermore, we can conclude that the itinerary of c_2 is $\overline{231}$.

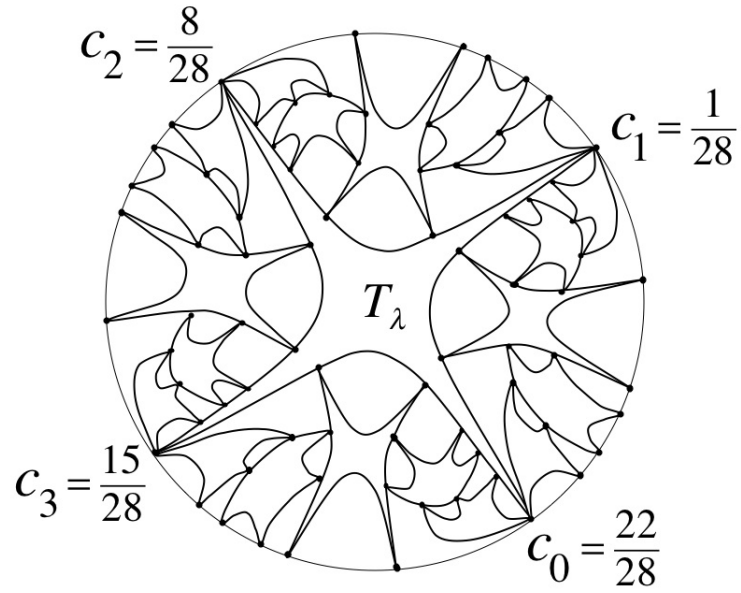


Figure 2.9: For the $\frac{1}{7}$ -Mandelbrot set, we use fourfold symmetry to extend the chain of preimages of the trapdoor into the other symmetry sectors.

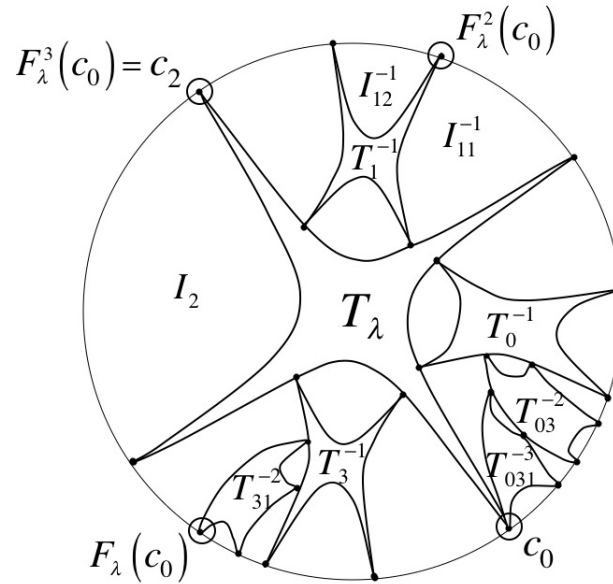


Figure 2.10: Given a model without the corresponding itinerary, we note that c_0 lies in I_{0312}^{-3} . Thus, c_2 is periodic with itinerary $\overline{231}$.

2.5 Conclusion

There is a rational parameter ray corresponding to each accessible Mandelbrot set. This rational angle corresponds to a unique itinerary for the periodic critical point of a map taken from center of the main cardioid of this Mandelbrot set. The itinerary determines the model for the Julia set of the map. Thus, each ray defines a unique model. Likewise, given a model, one can determine the unique corresponding itinerary. This allows us to conclude the following:

Theorem *For $n = d = 2$, given parameters λ and μ from the main cardioids of different accessible Mandelbrot sets, there exists a homeomorphism taking ∂B_λ to ∂B_μ and ∂T_λ to ∂T_μ if and only if $\mu = \bar{\lambda}$.*

In ongoing work, we consider cases of $n = d > 2$ and we conjecture that the same result will hold. We have found that, when n is odd, the construction of the models can be more challenging because there are always two periodic critical points. Sometimes these points lie on the same orbit of period $2n$ and other times each periodic critical point has a unique orbit of period n . Construction of these models is made easier by considering a map which is semi-conjugate to F_λ but has a single critical point.

We reiterate the distinction between our results those for the principal Mandelbrot sets. Each map taken from the main cardioid of a principal Mandelbrot set is known to have a Checkerboard Julia set. The Julia sets corresponding to maps taken from the main cardioids of distinct principal Mandelbrot sets are known to be homeomorphic and, in some cases, these maps exhibit conjugate dynamics on their Julia sets. In contrast, when we consider maps taken from main cardioids of distinct accessible Mandelbrot sets of period $m \geq 2$, we have seen that the corresponding

Julia sets cannot be homeomorphic and thus, such maps can never exhibit conjugate dynamics on their Julia sets.

Chapter 3

Construction of Models for $n = d \geq 3$

3.1 Locating Periodic Critical Points

When $n > 2$, we define parameter rays according to $\Phi(\lambda) = \phi_\lambda((F_\lambda(c_\lambda))^2)$.

Lemma 7: When $n = d \geq 3$, the external rays landing on accessible Mandelbrot sets in the upper halfplane correspond to rational angles of the form $\frac{t}{n^{m-1}}$ with $t = 1, 2, \dots, n^{m-1} - 1$. For $n = d$ odd, if λ is taken from the center of the main cardioid of the $\frac{t}{n^{m-1}}$ accessible Mandelbrot set, then c_{t+1} and c_{t+1+n} are the periodic critical points. Furthermore, when t is odd, both of these points lie on the same orbit of period- $2m$ and when t is even, these points lie on disjoint orbits of period- m . For $n = d$ even, if λ is taken from the center of the main cardioid of the $\frac{t}{n^{m-1}}$ accessible Mandelbrot set, then c_{t+1} is the periodic critical point with period- m .

Proof: The map $F_\lambda(z) = z^n + \frac{\lambda}{z^n}$ is conjugate to $z \mapsto z^n$ on B_λ which is conjugate to $\theta \mapsto n\theta$ on the exterior of the unit disk. Consider $\theta = \frac{t}{n^{m-1}}$ under $f(\theta) = n\theta$. $f^m(\theta) = n^m \left(\frac{t}{n^{m-1}}\right) = t + \frac{t}{n^{m-1}} = t + \theta$ where t is an integer. Thus $f^m(\theta) \equiv \theta \pmod{1}$.

The angle corresponding to c_1 is given by $\theta(c_1) = \frac{t}{2n(n^{m-1})}$. In general,

$$\theta(c_i) = \frac{t}{2n(n^m - 1)} + \frac{i-1}{2n} = \frac{t + (i-1)(n^m - 1)}{2n(n^m - 1)}.$$

We can then compute the angle corresponding to the m^{th} iterate of c_i under F_λ ,

$$\theta(F_\lambda^m(c_i)) = n^m \left(\frac{t + (i-1)(n^m - 1)}{2n(n^m - 1)} \right).$$

If $\theta(F_\lambda^m(c_i)) \equiv \theta(c_i) \pmod{1}$ (equivalently, if $\theta(F_\lambda^m(c_i)) - \theta(c_i) \in \mathbb{Z}$), then c_i has period- m under F_λ .

Suppose $i = t + 1$ and consider $\theta(F_\lambda^m(c_i)) - \theta(c_i)$

$$\begin{aligned} &= \frac{n^m(t + ((t+1) - 1)(n^m - 1))}{2n(n^m - 1)} - \frac{t + ((t+1) - 1)(n^m - 1)}{2n(n^m - 1)} \\ &= \frac{(n^m - 1)(t + t(n^m - 1))}{2n(n^m - 1)} \\ &= \frac{n^m t}{2n} \\ &= \frac{n^{m-1} t}{2}. \end{aligned}$$

Since $m \geq 2$ and $t \in \mathbb{Z}$, we see that, if n is even, then $\frac{n^{m-1}t}{2} \in \mathbb{Z}$, so c_{t+1} has period- m under F_λ . We know that all $2n$ of the c_i map onto the same point after two iterations, so c_{t+1} is the only periodic c_i .

On the other hand, if n is odd, then we can only be sure that $\frac{n^{m-1}t}{2}$ is an integer when t is even. However, if t is odd, then $\frac{n^{m-1}t}{2} \notin \mathbb{Z}$. But then $t+n$ is even. Consider the m^{th} iterate of c_{t+1+n} instead. \square

3.2 An Example with $n = d = 3$ and t odd

Consider the case of $n = d = 3$, $m = 3$, and $t = 1$. Since t is odd, we expect to have a single periodic critical orbit of period $2n = 6$, which contains two critical points, c_2 and c_5 . In this case, $\theta(\lambda) = \frac{1}{26}$ and $\theta(c_1) = \frac{1}{156}$. Then $\theta(c_2) = \frac{27}{156}$ has period-6

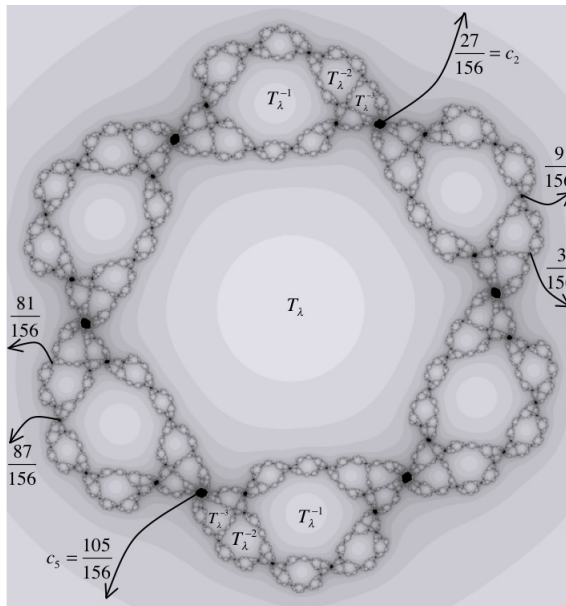


Figure 3.1: The Julia set for λ taken from the $\frac{1}{26}$ -Mandelbrot set when $n = 3$.

under tripling and maps to $\theta(c_5) = \frac{105}{156}$ after 3 iterations. One can compute that the corresponding itinerary is $S(c_2) = \overline{244511}$. However, since c_2 is a corner of T_λ and maps to c_5 , another corner of T_λ , after 3 iterations, we conclude that T_λ maps to itself after 3 iterations. Thus, the chain of preimages of the trapdoor consists of $\{T_\lambda, T^{-1}, T^{-2}, T^{-3}\}$. Figure 3.1 shows the Julia set for this case.

To construct a model of the chain of preimages, we know that $F_\lambda^5(c_2)$ lies in $\partial T_1^{-1} \cap \partial B_\lambda$ and is a preimage of c_2 the other two corners in $\partial T_1^{-1} \cap \partial B_\lambda$ must map to c_3 and c_4 and F_λ preserves orientation. Thus, we have located $F_\lambda^5(c_2)$ corresponding to the angle $\frac{9}{156}$ along ∂T_1^{-1} . Now $F_\lambda^4(c_2)$ is located in $\partial T_{11}^{-2} \cap \partial B_\lambda$ and must map onto $F_\lambda^5(c_2)$, so we can determine the arrangements of the corners of T_{11}^{-2} and locate $F_\lambda^4(c_2)$ corresponding to the angle $\frac{3}{156}$ on ∂T_{11}^{-2} . We can then make use of the symmetry of the map and the arrangement of the corners of T_{11}^{-2} to extend the model to I_2 and I_4 and to locate $F_\lambda(c_2)$ and $F_\lambda^2(c_2)$ corresponding to the angles $\frac{81}{156}$ and $\frac{87}{156}$, respectively.

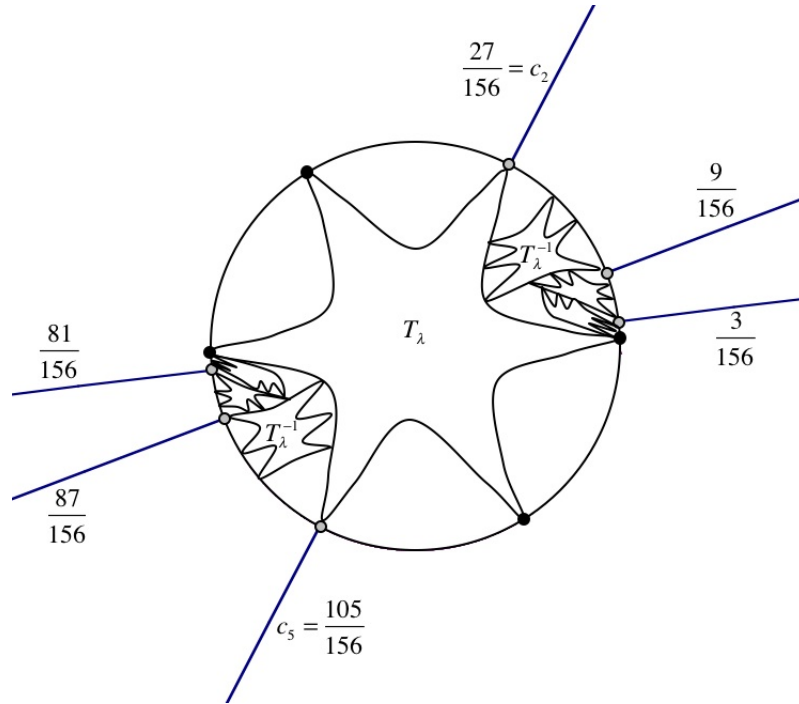


Figure 3.2: The model of the Julia set for λ taken from the $\frac{1}{26}$ -Mandelbrot set when $n = 3$.

Now, T_{244}^{-3} (having c_2 at one of its corners) maps onto T_{44}^{-2} such that $F_\lambda(c_2)$ is the rotation of $F_\lambda^5(c_2)$ by a half-turn about the origin (corresponding to the angle $\frac{81}{156}$). This gives us the arrangement of the corners of T_{244}^{-3} and completes our model. The model is shown in in Figure 3.2.

3.3 An Example with $n = d = 3$ and t even

Now consider the case of $n = d = 3$, $m = 3$, and $t = 2$. Since t is even, we expect to have a two disjoint periodic critical orbits of period $n = 3$, one containing c_3 and the other containing c_0 . In this case, $\theta(\lambda) = \frac{2}{26}$ and $\theta(c_1) = \frac{2}{156}$. Then $\theta(c_3) = \frac{54}{156}$ has period-3 under tripling. One can compute that the corresponding itinerary is $S(c_3) = \overline{311}$. Then, by symmetry, $S(c_0) = \overline{044}$. Thus, the chain of preimages of the

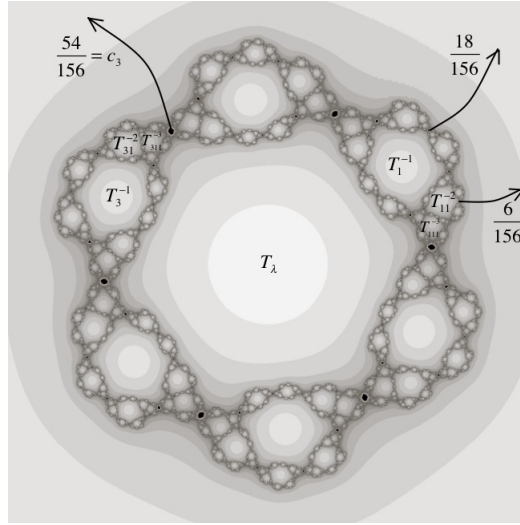


Figure 3.3: The Julia set for λ taken from the $\frac{2}{26}$ -Mandelbrot set when $n = 3$.

trapdoor again consists of $\{T_\lambda, T^{-1}, T^{-2}, T^{-3}\}$. Figure 3.3 shows the Julia set for this case.

3.4 Symmetries in the Parameter Plane

When n is even, there are an odd number of principal Mandelbrot sets in the parameter plane. These divide the connectedness locus into $n - 1$ sectors arranged symmetrically about the origin. One of the principal Mandelbrot sets will have its center on the positive real axis. This means that there is another sector which straddles the negative real axis. For each base period m , there are a total of $n^m - 1$ accessible Mandelbrot sets at the landing points of a ray of the form $\frac{t}{n^m - 1}$, where $t = 0, 1, 2, \dots, n^m - 2$. $n - 1$ of these are the principal Mandelbrot sets. The additional copies are divided evenly among the $n - 1$ sectors, giving a total of $n^{m-1} - n^{m-2} + n^{m-3} - \dots + n$ in each sector. This number is divisible by n , thus even. So each base period m accessible Mandelbrot set in the sector straddling the negative real axis is the complex conjugate

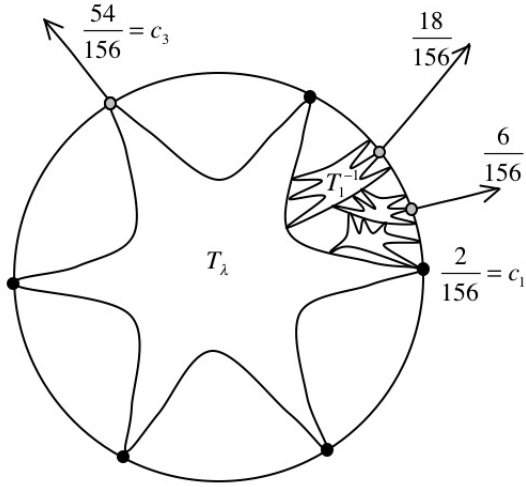


Figure 3.4: The model of the Julia set for λ taken from the $\frac{2}{26}$ -Mandelbrot set when $n = 3$.

of another such copy. As discussed in Section 1.3, we know that F_λ is dynamically conjugate to $F_{\bar{\lambda}}$. Thus, these complex conjugate pairs of accessible Mandelbrot sets produce maps that exhibit conjugate dynamics.

Furthermore, it can be shown that, when ω is an $(n - 1)^{st}$ root of unity, $F_{\omega^2\lambda}$ is dynamically conjugate to F_λ . For n even, any base period m accessible Mandelbrot set from another sector is conjugate to one in the sector straddling the negative real axis by a rotation of $\frac{k}{n-1}$ where $k \in \mathbb{Z}$. This means that there is a maximum of $\frac{n^m-1}{2(n-1)}$ conjugacy classes for maps of this type with base period m . In fact, it can be shown that these are there are exactly this many conjugacy classes when n is even. Using methods similar to those in Section 2.4, we can show that for any even n , homeomorphisms exist between Julia sets of F_λ and F_μ if and only if $\mu = \bar{\lambda}$ or $\mu = \omega^2\lambda$. As an example, Figure 3.5 displays the parameter plane for $n = d = 4$.

When n is odd, dynamical conjugacies are given by the same relationships, but because there are an even number of sectors in the parameter plane, we now get

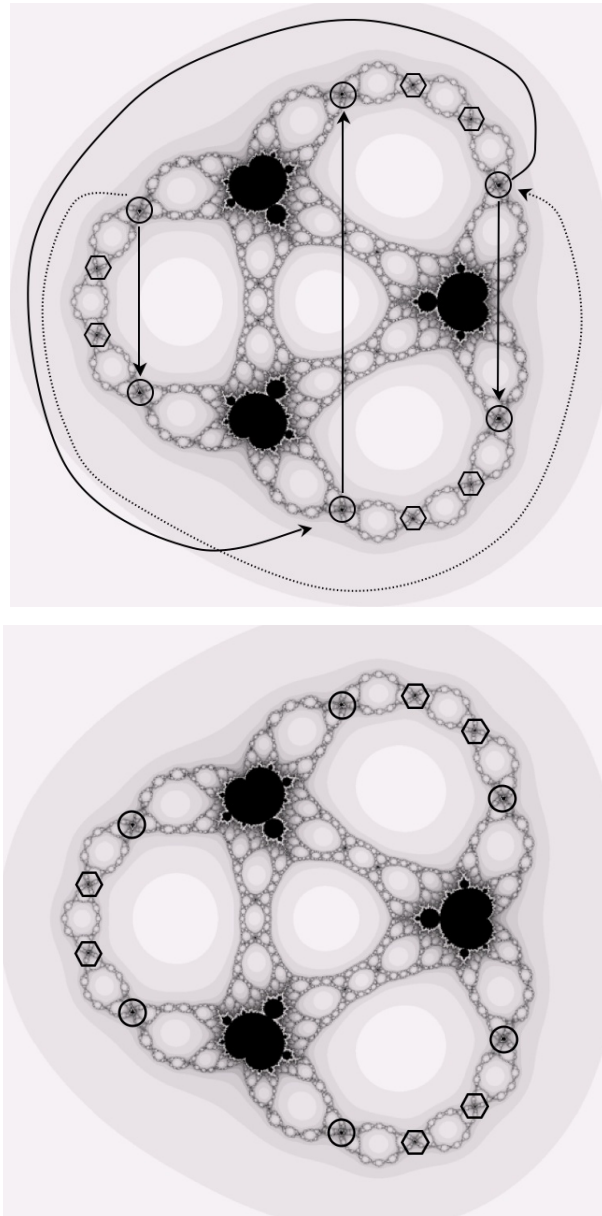


Figure 3.5: The parameter plane for $n = d = 4$. In the first image, arrows in the indicate dynamical conjugacies between maps taken from the centers of the main cardioids of the indicated period-2 accessible Mandelbrot sets. These conjugacies are given by complex conjugation and rotations. In the second image, we indicate all twelve period-2 accessible Mandelbrot sets. These comprise two conjugacy classes, one marked with circles and the other with hexagons.

additional conjugacy classes. The maximum number of conjugacy classes is now $\frac{n^m-1}{(n-1)}$. Figure 3.6 illustrates the case of $n = d = 5$. There are twenty period-2 accessible Mandelbrot sets. The eight indicated by circles all produce homeomorphic Julia sets. However, these are divided into two conjugacy classes, one indicated with white circles and the other indicated with black circles. Likewise, there are eight indicated by hexagons which all produce homeomorphic Julia sets but are divided into two conjugacy classes. Finally, there are an additional four indicated by squares which all produce homeomorphic Julia sets and comprise a single conjugacy class.

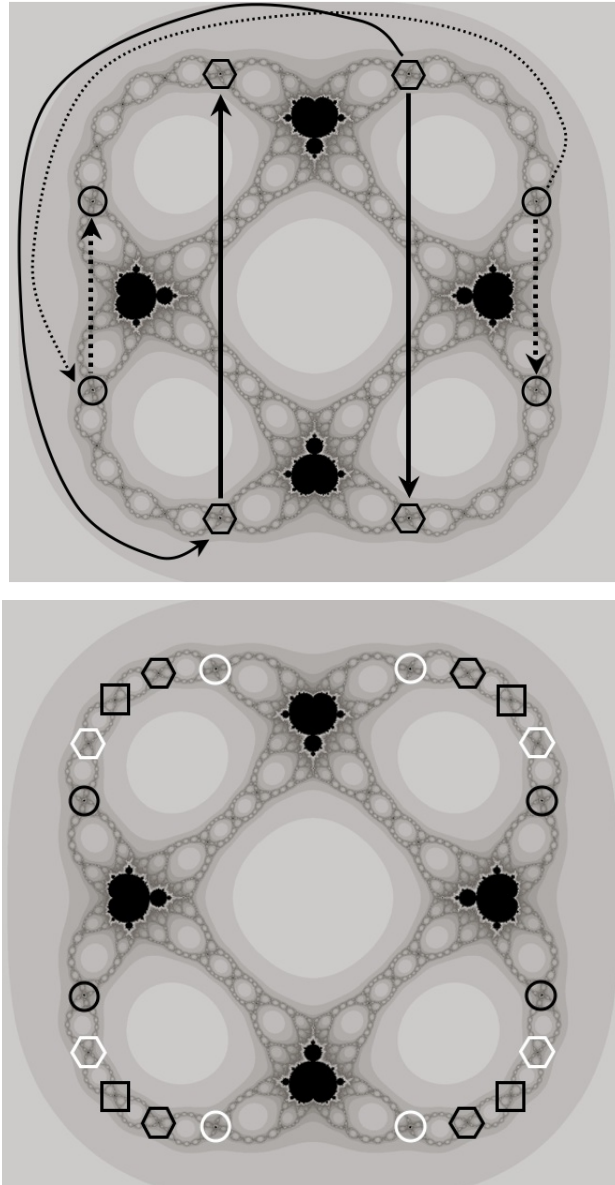


Figure 3.6: The parameter plane for $n = d = 5$. In the first image, arrows in the indicate dynamical conjugacies between maps taken from the centers of the main cardioids of the indicated period-2 accessible Mandelbrot sets. These conjugacies are given by complex conjugation and rotations. In the second image, we indicate all twenty period-2 accessible Mandelbrot sets and the five associated conjugacy classes.

Bibliography

- [1] P. Blanchard, F. Cilingir, D. Cuzzocreo, R. L. Devaney, D. Look, E. D. Russell, *Checkerboard Julia sets for rational maps*, International Journal of Bifurcation and Chaos in Applied **17** (2007), 131–148.
- [2] R. L. Devaney, *A myriad of Sierpiński curve Julia sets*, Difference Equations, Special Functions, and Orthogonal Polynomials. World Scientific, (2007), 131–148.
- [3] R. L. Devaney, *Baby Mandelbrot sets adorned with halos in families of rational maps*, Complex Dynamics: Twenty-Five Years After the Appearance of the Mandelbrot Set, American Mathematical Society. Contemporary Math, **396** (2006), 37–50.
- [4] R. L. Devaney, *A Cantor-Mandelbrot-Sierpiński tree in the parameter plane for rational maps*, Transactions of the AMS (to appear)
- [5] R. L. Devaney, D. Look, *Buried Sierpiński curve Julia sets*, Discrete and Continuous Dynamical Systems, American Institute of Mathematical Sciences **13** (2005), no. 4, 1035–1046.
- [6] R. L. Devaney, M. Moreno Rocha, S. Siegmund, *Rational maps with generalized Sierpiński gasket Julia sets*, Topology and its Applications. **154** (2007), no. 1, 11–27. doi: 10.1016/j.topol.2006.03.024
- [7] R. L. Devaney, D. Look, D. Uminsky, *The Escape Trichotomy for singularly perturbed rational maps*, Indiana University Mathematics Journal. **54** (2005), 1621–1634.
- [8] R. Mañé, P. Sad, D. Sullivan, *On the dynamics of rational maps*, Annales Scientifiques de l'École Normale Supérieure, Quatrième Série, **16** (1983), 193–217.
- [9] J. Milnor, *Dynamics in One Complex Variable*. 3rd ed. (Annals of Mathematics Studies, Princeton University Press, 2006)
- [10] C. Petersen, G. Ryd, *Convergence of rational rays in parameter spaces*, The Mandelbrot set: Theme and Variations, London Mathematical Society, Lecture Note Series 274, Cambridge University Press, (2000), 161–172.

- [11] W. Qui, P. Roesch, X. Wang, Y. Yin, *Hyperbolic components of McMullen maps*, Arxiv 1207.0266.
- [12] P. Roesch, *On capture zones for the family $f_\lambda(z) = z^2 + \frac{\lambda}{z^2}$, Dynamics on the Riemann Sphere*. European Mathematical Society, (2006), 121–130.

Curriculum Vitae

- Contact* Elizabeth L. Fitzgibbon (born 1980)
Department of Mathematics and Statistics, Boston University
111 Cummington Mall, Boston, MA 02215, USA
lizfitz@bu.edu
- Education* **Long Island University C. W. Post**
B.A., Mathematics for Secondary Education, February 2002.
M.S., Applied Mathematics, May 2005.
Boston University PhD candidate, September 2009 – present.
Thesis Advisor: Robert L. Devaney.
- Research Papers*
1. E. Fitzgibbon, S. Silvestri, *Rational Maps: Julia sets from accessible Mandelbrot sets are not homeomorphic.* (submitted 2013)
 2. P. Blanchard, D. Cuzzocreo, R. L. Devaney, E. Fitzgibbon, S. Silvestri, *A dynamical invariant for Sierpinski cardioid Julia sets.* (submitted 2013)
- Invited Talks*
- International Conference on Difference Equations and Applications.* Barcelona, Spain; July 2012. "Homeomorphisms between Julia sets of rational maps."
- 47th Spring Topology and Dynamics Conference.* Central Connecticut State University; March 2013. "Rational Maps: Julia sets from accessible Mandelbrot sets are not homeomorphic."
- Joint Mathematics Meetings, Special Session on Complex Dynamics.* Baltimore, Maryland; January 2014. "Rational Maps: Julia sets from accessible Mandelbrot sets are not homeomorphic."
- Invited Participant* *AMS Math Research Communities workshop on Complex Dynamics.* Snowbird Resort, Utah; June 2013.
- Posters* *Midwest Dynamical Systems Meeting.* University Illinois, Urbana-Champaign; November 2013. "Rational Maps: Julia sets from accessible Mandelbrot sets are not homeomorphic." With S. Silvestri.

*Teaching
Experience* **Syosset Central School District**
High School Mathematics Teacher
February 2001 – September 2009

Boston University

Instructor, Fall 2012 and Summers 2010–2014
Senior Teaching Fellow, RULE Calculus, Fall 2011
Teaching Fellow, September 2009 – May 2014
Summer Preview Instructor, Summer 2013
Tutor, PROMYS for Teachers, Summer 2013